The Interaction of Early Salt Stress-Induced 2 (ESI2) and the Ran G Protein in Arabidopsis

Alexandra Ralevski

A Thesis in the Department of
Biology

Presented in Partial Fulfillment of the Requirements for the Degree of Master of Science at

Concordia University
Montreal, Quebec, Canada

June 2013

CONCORDIA UNIVERSITY

School of Graduate Studies

This is certify that the thesis prepared

By: Alexandra Ralevski

Entitled: The Interaction of Early Salt Stress-Induced 2 (ESI2) and the Ran G Protein in Arabidopsis

and submitted in partial fulfilment of the requirements for the degree of

Master of Science (Biology)

Complies with the regulations of the University and meets the accepted standards with respect to originality and quality.

Signed by the final examining committee:

Dr. Dayanandan	Chair
Dr. Varin	Examiner
Dr. Storms	Examiner
Dr. Bachewich	Examiner
Dr. Gulick	Supervisor

Approved by

Dr. Dayanandan

Chair of Department or Graduate Program Director

Dean Brian Lewis

Dean of the Faculty of Arts and Science

Abstract

The Early Salt Stress-Induced 2 protein, ESI2, was identified as an interacting protein with the GTP-binding protein RAN via a His_6-tag pull-down assay and by bimolecular fluorescent complementation. Fluorescent protein fusions transiently expressed in *Nicotiana benthamiana* were observed using confocal fluorescent microscopy. The proteins fused to independent fluorescent partners localized to separate cellular compartments, with RAN primarily localized to the nucleus and ESI2 localized primarily to the tonoplast and cytoplasm. This interaction suggests a potential mechanism for the role of ESI2 in the sequestration of RAN and possible regulation of cell division in response to stress. To further explore the role of ESI2, the protein was overexpressed in *Arabidopsis* however plant phenotypes were not found to differ from wild type plants.

Acknowledgements

Working on this thesis, I have learnt a great deal from those around me. The experiences I have gained have given me great confidence and motivation to further myself and my career. This would not have been possible without the help of my colleagues, supervisor, and family.

First, my sincerest appreciation goes to Concordia University, for giving me both the opportunity to further my education, and providing me with the resources to succeed. The knowledge and memories I have gained though my experiences at this institution I hold very dear to me and will treasure for years to come.

I would also like to thank my colleagues, especially Sabrina Brunetti, without whom the completion of this thesis would not have been possible.

The sincerest of thanks also goes my supervisor, Dr. Gulick, who remains one of the most patient and understanding people I have ever known. His continual guidance and support allowed me to stay focused and gave me the confidence I needed to see this thesis through.

Finally, I owe my deepest thanks to my family. Their constant patience, encouragement, and support have been irreplaceable. It is from them that I get my strength that has brought me to this point, and will continue to guide me throughout my future.

Table of Contents

List of Figures

PART I. INTRODUCTION

The driving force behind agriculture is an ever-increasing demand for food to sustain a rapidly growing global population. This pressure to continually grow more crops in a wider variety of environments further drives the need for scientists to design and develop more stress-resistant crop plants. Crops that can endure the effects of exposure to multiple abiotic or biotic stresses while maintaining fecundity will prove to be the most useful for farmers operating in the growing global agricultural market.

The effects of stress on the proper development and growth of plants currently poses a severe threat to agriculture. Crop production worldwide is consistently faced with a wide range of inimical stresses that threaten global food production and decrease agricultural productivity. Overall, it is estimated that abiotic stresses reduce the average yields for most major crop plants by up to 50% (Bray *et al.* 2000). Water shortages due to drought are a major problem for 45% of the world's lands, where 38% of the human population lives (Chinnusamy *et al.* 2008). Salinization in the soil is predicted to cause up to a 50% reduction in arable land by the year 2050 (Pitman and Läuchli 2002). Additionally, stress on plants induced by high temperatures is said to affect about 40% of irrigated areas of wheat (Chinnusamy *et al.* 2008). Global warming and climate change is predicted to only further exaggerate and intensify these already numerous and severe limitations to plant growth.

However, despite the seemingly endless onslaught of harmful stresses, plants have evolved an intricate and complex stress response system to counter-act harmful environmental stresses. Precise recognition of external stresses and subsequent orchestration and activation of genes involved in stress-related responses are crucial for

the sustained survival and proliferation of plants living in hostile environments. Plants have developed a variety of stress response pathways, many of which can be overlapping if the stress is pleiotropic, or if multiple stresses are coupled together. The most common responses take the form of cell-signalling cascades that result in a modification of the transcriptome. This in turn can lead to decreased cell growth and cell division, reduced photosynthesis and increased stomatal closure, among other responses (Knight and Knight, 2001).

Triticum aestivum, more commonly known as bread wheat or common wheat, is one of the major cereals used as a source of food for nearly one fifth of the world's population (Food and Agriculture Organisation of the United Nations, 2012). One way to ensure the continual productivity of this vital crop would be to fully elucidate the mechanisms and pathways that function to control the stress response in wheat. This would enable scientists to engineer more resistant and viable agricultural crops, eventually securing the future production of this essential food. In general, a deeper and more thorough understanding of the genes involved in the plant stress response will help further our understanding of how we can improve the productivity of crop plants growing in adverse environments.

1. Gene Candidate Identification

In wheat, genes that differed in expression levels between cold-acclimated spring and winter cultivars were identified as potential regulatory or signalling proteins in the cold stress response (Gulick *et al.* 2005). These genes were then used as bait in a Yeast Two-Hybrid screen to identify other genes involved in the stress response in wheat, and to

subsequently build a map of protein-protein interactions (Tardiff *et al.* 2007). One of the genes used as bait, a cold-induced G-RAN-like protein, was shown to interact with the previously identified Early Salt Stress-Induced 2 (ESI2) protein (Tardiff *et al.* 2007, Galvez *et al.* 1993).

2. The Wheat Esi2 Protein

Esi2 is a unique gene in its response to stress. It is highly expressed in wheat cultivars that were the most freeze-tolerant, including Musketeer, which has an LT_{50} of -21ºC (LT_{50} is the temperature at which 50% of plants will survive) and Norstar, which has an LT_{50} of -19ºC. It also showed reduced levels of expression in the more cold-sensitive spring wheat varieties of Glenlea (LT_{50} -8ºC), and Concorde (LT_{50} -8ºC) (Unpublished, Gulick). It was also shown to be up-regulated after the initiation of salt stress in *L. elongatum* (Gulick and Dvorak 1992). *Esi2* is characterized by a copper-binding domain and a region consisting of repeating amino acid motifs that are high in methionine, proline, and serine, which as yet bears little resemblance to other stress-response genes outside of the Triticale tribe.

3. The Ran Protein

Ran is a small GTPase and member of the Ras superfamily of proteins. Like other G proteins, Ran switches from an "active" GTP-bound state and an "inactive" GDP-bound one. The Ran accessory proteins RanGAP1 and the GDP/GTP exchange factor, RCC1, aid in this GTP hydrolysis and activation, respectively. It has long been known that Ran is a vital and indispensable enzyme responsible for orchestrating numerous

critical aspects of cellular function such as mitotic progression, spindle assembly, and nucleo-cytoplasmic transport (Dasso 2002).

Gene expression and regulation are controlled post-transcriptionally in higher organisms, a key feature distinguishing them from their prokaryotic counterparts. A well-defined barrier between the nucleus and the cytoplasm places enormous emphasis on gene regulation and control via nucleo-cytoplasmic trafficking, including pre-mRNA processing, mRNA stability, mi/siRNA export from the nucleus, and translation. This trafficking therefore has great control over gene regulation in response to environmental stress. Ran is one of the key genes involved in the shuttling of "cargo" (proteins, tRNA, miRNA/siRNA, etc) into and out of the nucleus, and interacts with nuclear transport receptors from the karyopherin/importin β family of proteins (Chinnusamy *et al.* 2008), as well as the importin α family, part of the ARM repeat protein family (Merkle 2011). In contrast, the transport of mRNAs is mediated by the non-karyopherin family of NEFs. Karyopherin-mediated transport is tightly controlled by an asymmetric Ran gradient across the nuclear envelope, maintained by the RanGEF, RCC1, in the nucleus, and the RanGAP, RanGAP1, aided by RanBP1/2, in the cytoplasm. For entry into the nucleus, cargo must contain a nuclear localization signal (NLS), which is recognized by a NLS-binding domain on importin α. Importin β binds the cargo/importin α pair and the completed complex shuttles across the perinuclear space through a nuclear pore complex (NPC). Once inside the nucleus, RanGTP binds importin β and dissociates the complex, thereby releasing the cargo. RanGTP-bound importin β is free to shuttle back to the cytosol where RanGTP is hydrolyzed back to RanGDP. RanGTP also binds importin α as well as the exportins Exportin2 and CAS to facilitate nuclear exit (Dasso 2001,

Chinnusamy et al. 2008). RanGDP is separately shuttled into the nucleus by NTF2 (Nuclear Transport Factor 2), which binds to GDP-bound Ran in the cytoplasm and inhibits dissociation of GDP from Ran (Görlich and Kutay 1999). Since the intrinsic rate of Ran's nucleotide exchange and hydrolysis are slow (Görlich *et al.* 2003), nucleo-cytoplasmic transport is thus hypothesized to be driven by an asymmetric distribution of the Ran effectors: RanGTP levels are kept high in the nucleus by abundant chromatin-bound RCC1, and RanGAP1 promotes quick GTP hydrolysis in the cytoplasm, freeing RanGDP to associate with NTF2 and shuttle back to the nucleus to continue the cycle.

Ran has also been known to play a critical role during the cell cycle. In mammals, following nuclear envelope breakdown, a gradient of RanGTP extends centrifugally from the centrosomes (Hasegawa *et al.* 2013). This high concentration of RanGTP is again maintained by RCC1 and the counter-acting force of RanGAP1, allowing for Ran-GTP-dependent factors such as Ran-BPM to stimulate microtubule assembly near the chromosomes (Kahana and Cleveland 1999). The activated GTPase can also stimulate microtubule aster formation by binding importins and allowing the release of microtubule-nucleating factors such as NuMa and TPX2 (Gruss *et al.* 2001). Asters surround the centrioles, the sites from which microtubules emanate. Microtubules then connect to the kinetochore of each chromosome and direct their movement to facilitate chromosome alignment along the metaphase plate.

Plant cell division differs from its mammalian counterpart in that it does not require the use of centrioles to direct spindle assembly. This "spindle self-assembly" was shown to also function independently of the preprophase band (PPB) (Zhang and Dawe 2011), a critical cell marker during G2 phase which defines the future site of cortical

division (CDS) and which is thought to act as a guide for the growing phragmoplast (Xu *et al.* 2008). Consequently, it has now been hypothesized that chromatin, in conjunction with a Ran-dependent pathway, are sufficient for spindle formation in plant cells, further emphasizing the importance of Ran in the plant cell cycle.

3.1 Ran in Response to Stress

The role of Ran in response to stress is an area of research that is still in its early stages. A study done by Wang *et al.* in 2006 showed that overexpression of the wheat Ran, Ta-*Ran1*, in Arabidopsis and rice exhibited an increase in the number of cells in the G2 phase of the cell cycle, which resulted in an elevated mitotic index and extended life cycle. Overexpression of Ta-*Ran1* also led to increased primordial tissue, reduced number of lateral roots, and stimulated hypersensitivity to exogenous auxin. In 2010, Zang *et al.* did a similar study on *OsRan2*, a Ran gene from rice. They revealed that expression of the Ran gene in rice was reduced under salt and osmotic stress, as well as exogenous treatment of ABA. Additionally, overexpression of *OsRan2* in transgenic Arabidopsis and rice showed hypersensitivity to osmotic stress, salinity, and ABA stress. A study done in 2001 by Kim *et al.* showed that antisense expression of RanBP1 in Arabidopsis resulted in plants with prematurely terminated lateral roots, but enhanced primary root growth. When treated with auxin, the transformed plants exhibited hindered mitotic progression in newly emerged lateral roots and the primary root tip. Taken together, it is evident that another role for Ran has emerged, this time as a possible regulator of plant cell functioning and development in response to stress.

3.2 The Arabidopsis Ran

The Arabidopsis genome has four RAN homologs termed At-*RAN1* (At5g20010), At-*RAN2* (At5g20020), At-*RAN3* (At5g55190) and At-*RAN4* (At5g55080). At-*RAN1*, *2* and *3* were first characterized by Haizel *et al.* in 1997. The authors revealed that At-*RAN1* and At-*RAN2* contained five exons and four introns, while At-*RAN3* contained eight exons and seven introns. They also deduced that the amino acid sequences of the three genes were nearly identical, differing from each other only at the C-terminal regions, and that each protein consisted of 221 amino acid residues. At-*RAN4* was characterized by Vernoud *et al.* in 2003, and was shown to share only 65% of its identity with the other three Arabidopsis *RANs*. It was also reported that there is a highly conserved sequence motif (KKYEPTIGVEV) shared between At-*RAN1*, *2* and *3*, that acts as a site for GTP binding and hydrolysis, as well as an interaction domain for RanGAPs. At-*Ran4* only has five of these eleven residues conserved (Vernoud et al. 2003). Additionally, Arabidopsis *RAN1*, *2* and *3* share 94% identity and 95% similarity to the wheat *Ran* gene homolog (Benson *et al*. 2005).

4. *Arabidopsis thaliana* and *Triticum aestivum*

By the 1980's a mini-revolution had begun in plant genetics. *Arabidopsis* was chosen over petunia, tomato, and several other plants as the model organism for plant molecular biology. It had many traits that appealed to plant geneticists, including a small genome (5 chromosomes) which facilitated gene cloning and gene identification, a short generation time (28 days from germination to flowering), high seed production (10,000 plus seed per plant), and it was easy to create embryo lethal, morphological, life-cycle,

and hormone response mutations (Meyerowitz 2001). With the addition of a fully sequenced genome (The Arabidopsis Genome Initiative 2000), as well as stocks of T-DNA insertion mutants for every gene (Alonso *et al.* 2003), *Arabidopsis thaliana* has not only lived up to expectations as the model organism for plant biology, it has well surpassed them.

The bread wheat *Triticum aestivum* is an allohexaploid (an allopolyploid with six sets of chromosomes, two sets from each of three different diploid donor species), and is the result of two interspecific hybridization events that occurred in conjunction with polyploidization. The first hybridization event occurred between 0.5 and 3 MYA, and combined the genomes of *Triticum urartu* (AA) and an unidentified species (BB) to produce the allotetraploid genome of *Triticum turgidum* (AABB) (Berkman et al. 2013, Chantret *et al.* 2005). The second event combined the genomes of *T. turgidum* (AABB) and *Aegilops tauschii* (DD) to produce the allohexaploid genome of *T. aestivum* (AABBDD) (Berkman *et al.* 2013, McFadden and Sears, 1946). Despite its usefulness as an edible crop, the bread wheat genome has proven difficult to sequence due to its large size, 80 – 90% of which is repetitive (Wanjugi *et al.* 2009). However, *T. aestivum* has adapted to a wide range of environmental conditions and has evolved to be extremely cold-tolerant, with some cultivars able to survive temperatures as low as -22ºC after a period of cold acclimation.

5. Fluorescent Proteins

5.1 GFP and Derivatives

The discovery of the green fluorescent protein (GFP) for use in scientific research has been heralded as one of the greatest discoveries in modern science. Its limits as a scientific tool for cell visualization in real-time seem boundless, and its applications far-reaching. The discovery of GFP earned Osamu Shimomura, Martin Chalfie and Roger Tsien the Nobel Prize in Chemistry in 1998 (Zimmer 2009). Purified GFP, or wild type GFP (wtGFP) is comprised of 238 amino acids consisting of an 11-stranded β-barrel encasing a central helix (Ormö *et al.* 1996). Fluorescent blue light is produced when calcium binds the photoprotein aequorin. This light undergoes radiationless energy transfer to GFP, which finally emits the now famous green light (Zimmer 2009). However, the version of GFP most commonly used in the laboratory today is not wtGFP, as it posed complications and the amino acid sequence has since been modified. The more improved version and the one most commonly used today is enhanced GFP (eGFP). Unlike its predecessor, eGFP emits a single excitation peak at 488 nm, as opposed to the double peaks of wtGFP at 395 and 475 nm. This was achieved by a single point mutation, S65T (Heim *et al.* 1995). Additionally, wtGFP exhibits poor folding at 37ºC and is sensitive to chloride and pH, all drawbacks that have been improved upon in the eGFP version.

The discovery of GFP has set off a search for other fluorescent proteins of different colours, so that it is possible to view two or more proteins together in the same field of view. One of the most common derivatives of wtGFP is the enhanced yellow fluorescent protein, (eYFP), previously known as YFP 10C (Shi *et al.* 2007). The other

most common fluorescent proteins are DsRed and mCherry, although these are not derivatives of wtGFP; they were originally isolated from the mushroom coral *Discosoma* (Li *et al.* 2008). Originally, DsRed posed problems for cell imaging as it formed a dimer in its natural state. mCherry is an improved derivative of DsRed with five amino acid substitutions (Q66M, T147S, M163Q, M182K, T195Q) (Shaner *et al.* 2004). Additionally, since it has an excitation maximum at 587 nm, and an emission maximum at 610 nm, in can be used concurrently with eGFP for the observation of two fluorescent proteins simultaneously.

5.2 Cloning into pFAST Vectors

The pFAST vectors carry a selectable marker which produces GFP that can be seen exclusively in the seed of transgenic plants. The marker was constructed as a fusion protein of OLE1 and eGFP, under the control of the OLE1 promoter, pOLE1 (Shimada *et al.* 2010). OLE1 is the most common oleosin in Arabidopsis, a protein that surrounds seed oil bodies. Oil bodies contain reserves for the germination and post-germination growth of seedlings. Oleosins are essential for stabilization of oil bodies (Huang 1996), as well as protecting the seed against damage incurred by freezing and thawing of cells (Shimada *et al.* 2008). In the pFAST vectors, the promoter of OLE1 controls the expression of a fusion protein of OLE1 oleosins expressing GFP, which functions as a selectable marker to identify transgenic seed via green fluorescence in the seed coat. GFP expression is limited to only the oil bodies of dry seeds, and fades completely five days after the germination of the seed (Shimada *et al.* 2010). The transgenic seed can be detected under a fluorescent microscope, and authors claim that homozygous seed may be detectable as the brightest seed within the T_2 generation. The quick detection of rare

transformants in T_1 seed and easy determination of the number of independent gene insertions in each line, as well as the rapid identification of homozygotes in the T_2 generation without the need for selection of transgenic seedlings with antibiotics, has made the pFAST vector a useful tool in the creation and detection of transgenic plants.

5.3 Bimolecular Fluorescent Complementation

One of the easiest and most reliable methods for determining a protein-protein interaction in plants is Bimolecular Fluorescence Complementation (BiFC). This method is based on the fact that certain fluorescent proteins remain stable if they are truncated at certain resides into two halves. One example of these proteins is the yellow fluorescent protein, eYFP. This protein has been modified and split into two "halves", the N-terminal half, (YN154, amino acid residues 1-154) and the C-terminal half (YC155, amino acid resides 155-238) (Hu *et al.* 2002). To test an interaction between two candidate proteins, each candidate is fused to one half of the YFP protein by subcloning the genes for these proteins as fusions in plant expression vectors for expression in tobacco cells. If the two proteins do indeed interact, the two halves of the YFP will reconstitute a fluorescent product that can be visualized using fluorescence microscopy. Because the detection of the interaction is sensitive, the location and level of fluorescence within the cell is a reliable indication of protein-protein interactions within an organism. In this thesis, BiFC was used to test the interaction of various proteins using *Agrobacterium tumafaciens* for transient transformation into *Nicotiana benthamiana* epidermal leaf cells (Sparkes *et al.* 2006).

6. Summary

The purpose of this thesis is to explore the role of the *ESI2* gene in the plant stress responses of *Arabidopsis* and *Triticum aestivum*. The identification of the interaction of *ESI2* with G-*RAN* suggests that it plays a role in regulation and signalling. Expanding the study of *ESI2* to *Arabidopsis* is an opportunity to use the extensive genetic resources that are available in the model system. The *RAN* gene has been shown to be vital in several aspects of cell-cycle control, and more recent experiments have revealed its role as an important regulator of the plant stress response. Genes that regulate or are regulated by *RAN*, such as *ESI2*, are excellent candidate genes for studying the stress response. Experimentation will reveal where these two genes localize and interact in cells, as well as the phenotypic outcome of the overexpression of the *ESI2* gene.

PART II. MATERIALS AND METHODS

1. Vector Constructs

The wheat Esi2 His_6-tag fusion gene construct was made previously in our laboratory using primers N02*att*B1 and N02*att*B2 (shown in Table 1). The PCR product was then inserted into the pDONR201 Gateway vector (Life Technologies) and the resulting entry clone was then sub-cloned into the Gateway pDest17 (Life Technologies) expression vector to obtain an N-terminal His_6 tagged protein for expression in *E. coli*.

The wheat Ran GST-tag fusion gene construct was also made previously in our laboratory, and was cloned into the Gateway pDest15 expression vector (N-terminal GST-tag *E. coli* expression vector, Life Technologies) using the primers RlGBattB1F and

RlGBattB1R (shown in Table 1) and the same cloning method described for the wheat Esi2 .

At-*ESI2* cDNA stock, (DKLAT4G27520), corresponding to an Arabidopsis gene (AT4G27520.1) with sequence similarity to the wheat gene, Ta-*Esi2*, was obtained as a bacterial stab from the Arabidopsis Biological Resource Center at Ohio State University. It was PCR amplified using the primers AtESI2FPGW and AtESI2RPGWstop or AtESI2RPGWnostop (shown in Table 1) and then incorporated into the pDONR201 Gateway vector (Life Technologies) by the BP *in vitro* recombination reaction according to the manufacturer's instructions. The subsequent entry clone was then inserted into the eGFP vector with a full length C-terminal eGFP fusion (pK7FWG2.0, Karimi *et al.* 2002), for GFP visualization to determine localization of At-*ESI2* in tobacco cells. The eYFP-C vector (pBatTL-B-sYFP-C) was used to create a C-terminal fusion of the C-terminal fragment of YFP with the Ta-*Esi2* and At-*ESI2* genes, and the eYFP-N vector (pBatTL-B-sYFP-N) was used to create a C-terminal fusion of the N-terminal fragment of YFP, with the Ta-*Ran* and At-*RAN* genes to study protein-protein interactions via BiFC in tobacco. At-*ESI2* was also inserted into the pFASTG02 vector (p*7FWG2, Plant Systems Biology), for overexpression of the At-*ESI2* gene under the control of the cauliflower mosaic virus (CaMV) 35S promoter (Karimi *et al.* 2002). This pFAST vector, as well as those mentioned below, all carry a screenable marker which produces a GFP signal visible in the mature seed coat of transformed plants. The three pFAST vectors are Gateway compatible, and the cloning was done according to the manufacturer's instructions by first inserting the DNA of interest into the entry vector pDNOR201, and subsequently transferring the clones into the specific pFAST vectors by *in vitro*

recombination. At-*ESI2* was also cloned into the pFASTG03 vector (p*7GWIWG2(I), Plant Systems Biology) which produces a double-stranded RNA (hairpin RNA), triggering post-transcriptional gene silencing under the control of the CaMV 35S promoter (Wesley *et al.* 2001, Karimi *et al.* 2002). The pFASTG04 vector (p*GWFS7, Plant Systems Biology) is used to fuse an experimental plant gene promoter with *EgfpER* and β-glucuronidase (GUS) (Karimi *et al.* 2002), for expression of the GUS reporter gene. The primers used for PCR amplification of the At-*ESI2* promoter were AtESI2GUSFP and AtESI2GUSRP2 (shown in Table 1).

2. Protein Purification and Protein-Protein Interaction

For protein-protein interaction characterization, *E. coli* BL21 cells transformed with the recombinant plasmids were grown at 37ºC in 500 mL LB media with 50 μg/ml spectinomycin for 6 h and then induced with 1 mM IPTG and incubated for 12 h at room temperature. Cultures expressing TaEsi2-GST (pDest15) were lysed in buffer: 50mM Tris-HCl, pH 8.8, 100mM NaCl, 2% Triton X-100, 5% Glycerol, and 1mM PMSF. The recombinant Ta-Esi2-GST protein was purified with Glutathione Sepharose™ according to the manufacturer's protocol (GE Healthcare Life Sciences). Cultures expressing Ta-Ran-His_6 (pDest17) were lysed in the same buffer, centrifuged at 12,000g for 15 min, and protein was recovered from the pellet by solubilization in buffer: 50mM Tris-HCl, 0.5% SDS, 5% Glycerol, and 1mM PMSF. Ta-Ran-His_6 was purified using Ni-NTA Agarose (Qiagen) according to Todorova (2009) with some modifications: the Ni-NTA Agarose was equilibrated with wash buffer containing 50mM Tris-HCl, pH 8.8, 0.05% SDS, and 1mM PMSF. The protein was immobilized on the equilibrated beads, rinsed twice with

wash buffer, and then eluted with 2X-SDS-PAGE buffer (100 mM Tris·HCl (pH 7.0), 200 mM DTT, 4% (W/V) SDS, 0.2 % (W/V) Bromophenol Blue, 30% glycerol, and 100 mM Imidazole).

The His_6-tag pull-down assay (Todorova 2009) was used to study the pair-wise interaction between Ta-Esi2-GST and Ta-Ran-His_6. A mixture of 50 µl of crude extract of the Ta-Ran-His_6 culture and 50 µl of Ni–NTA Agarose beads, previously equilibrated with the wash buffer (50mM Tris-HCL, 400mM NaCl, 5% glycerol, 1mM PMSF), were incubated for two hours at 4°C with gentle shaking. The mixture was rinsed with the wash buffer, centrifuged at 2000g for 1 min, and the supernatant was discarded. To assay the GTP/GDP bound forms of Ta-*Ran*, lysate was pre-treated with 5 mM EDTA and 5 mM of either GDP or GTP for 10 min followed by the addition of 20 mM $MgCl_2$. The Ni–NTA Agarose beads bound with either GTP or GDP-bound forms of Ta-Ran-His_6 protein were incubated with 1 ml of Ta-Esi2-GST crude *E. coli* lysate in 50mM Tris-HCl, pH 8.8, 100mM NaCl, 2% Triton X-100, 5% Glycerol, 1mM PMSF overnight at 4°C with gentle shaking. Samples were centrifuged at 2000g, washed twice with wash buffer, and then eluted in 50µl of 2X-SDS-PAGE buffer, boiled for 5 min at 100ºC, and analyzed by SDS-PAGE electrophoresis on 12% polyacrylamide gels subsequently stained with Coomassie Brilliant Blue R-250.

3. Agrobacterium-mediated Transformation of *Arabidopsis thaliana*

Three Arabidopsis plants were used for transformation according to Bent (2006) with the pFASTG02 vector for overexpression of the At-*ESI2* gene under control of a 35S promoter (35S:AtESI2). 35S::AtESI2 in the pFASTG02 vector was transformed into the

Agrobacterium tumafaciens strain AGL1 via electroporation and colonies were selected on LB media plates with 50μg/ml spectinomycin. Single colonies were picked and cultured in LB media with 50μg/ml spectinomycin and grown to OD_{600} = 0.6. The cultures were then centrifuged at 13,000g for 30 minutes and the pellets were re-suspended in a 5% sucrose solution. Plants were dipped according to Clough and Bent (1998) with the following modifications: Silwett L-77 was added to the sucrose solution to a concentration of 0.05% and *Arabidopsis* plants with emerging flower stems were dipped in the solution for five seconds. The plants were then kept in the greenhouse under transparent covers with 16 hr light and 8 hr dark at 22 °C, for several days. Covers were removed and plants were grown until seed was mature. Sees were collected and screened for transgenic individuals by the expression of the green fluorescence protein in the seed coat by fluorescence microscopy under 100X magnification with the Zeiss Axioplan fluorescence microscope (Carl-Zeiss, Germany). Transgenic seeds were sown in soil mixture containing equal parts of black earth, peat moss, and vermiculite that was pre-heat treated at 150°C for three hours. Seeds were then stratified in the dark at 4°C for 3-4 days. Pots were then placed in growth chambers and seedlings were grown at 22°C, 43.21 $\mu mol \cdot m^{-2} \cdot s^{-1}$ fluorescent light, with a light cycle of 16 hr light and 8 hr dark.

4. Screening and Identification of Transgenic *Arabidopsis* seed

A transgenic seed can be identified by green fluorescence, which is carried as a selectable marker in the pFAST vectors. Of the three plants treated with *Agrobacterium,* only one produced transgenic seeds. From this plant, twenty-three transgenic seeds exhibiting eGFP expression were collected and grown to produce T_2 seeds. T_2 seeds

collected from these plants were observed for eGFP expression under the fluorescence microscope. Lines with a single transgene insertion were identified by a 3:1 segregation ratio of GFP to no-GFP, respectively. Lines with at least two insertions were identified by a segregation ratio of at least 15:1 of GFP to no-GFP, respectively. Transgenic seed exhibiting eGFP expression from twenty of the twenty-three lines were again selected and grown to the next generation. Lines 3-7, 12-2, and 3-12 were used for phenotypic analysis of transgenic plants grown in soil. Ten plants from each of the homozygous transgenic lines, as well as ten wild type Columbia plants, were grown in soil conditions described above. Time to germination, time to flowering, and leaf number at flowering were recorded for each plant.

5. Agrobacterium-mediated Transient Transformation of *Nicotiana benthamiana*

Wild tobacco (*Nicotiana benthamiana)* were grown for four or five weeks in a soil mixture of 1:1:1 of black earth, vermiculite, and peat moss at 22ºC, 43.21 $\mu mol \cdot m^{-2} \cdot s^{-1}$ fluorescent light, with a light cycle of 16 hr light and 8 hr dark and covered with transparent plastic domes to increase humidity and ease of transformation.

Ta-Esi2*::C*-YFP, Ta-Ran*::N-YFP,* At-ESI2*::C-YFP*, At-*ESI2::eGFP*, At-RAN:N-YFP, At-RAN::eGFP, the tonoplast marker (gammaTIP::mCherry, Nelson *et al.* 2007), and p19 containing the vector for suppression of gene silencing (Voinnet *et. al* 2003) were transformed into the *Agrobacterium tumafaciens* strain AGL1 via electroporation and colonies were selected on LB media plates with the appropriate antibiotic. Single colonies were picked and cultured in LB media with the appropriate antibiotic to an OD_{600} of 0.6. The cultures carrying appropriate clones for each desired protein-protein

interaction that were to be assayed were mixed, along with the p19 containing culture, and mixtures were then pelleted by centrifugation at 6,000 rpm for 20 minutes at room temperature. The pellets were then re-suspended into an activating solution containing 1.5 mM acetosyringone and 0.01M $MgCl_2$ (English *et al.* 1996). Each mixture of cultures was then taken up in a syringe, without a needle, and injected directly into the underside of a tobacco leaf (Sparkes *et al.* 2006). Fluorescent interactions were visualized using the Leica TCS SP2 microscope system from the Center for Structural and Functional Genomics. A 488 nm and 543 nm laser scanner was used to excite the eGFP/eYFP and mCherry proteins, respectively. The mCherry cellular markers used were the tonoplast marker (vac-rk CD3-975), and plasma membrane marker (pm-rk CD3-1007) (Nelson *et al.* 2007).

6. RT-PCR of pFASTG02 35S::AtESI2 overexpression lines

Arabidopsis plants were grown for three weeks in the soil conditions described above for tobacco. Total RNA was extracted from *Arabidopsis* using the RNeasy Plant Mini RNA extraction kit (Qiagen) and a portion of the total RNA was reverse-transcribed using oligo(dT)-primed cDNA synthesis. One µg of total RNA and 3µl of 50 mM oligo(dT) were combined and heated at 70°C for 5 min, and cooled on ice. The RNA was then incubated with 0.9 mM dNTPs, 1X RT buffer and 20 units of M-MuLV reverse transcriptase in a 22 µl reaction volume using the temperature regime: annealing at 37°C for 5 min, cDNA synthesis for 60 min at 40°C and for 20 min at 55°C, and denaturation for 10 min at 70°C. PCR amplification of an aliquot of the cDNA to determine levels of gene expression was done using primers AtESI2cDNAFP1 and AtESI2cDNARP1 and

reaction conditions with initial denaturation at 95°C for 5 min followed by 25 cycles of denaturation at 95°C for 60 s, annealing at 55 °C for 40 s and extension at 72°C for 60 s. The same PCR assay was also done with 27 and 30 cycles of amplification.

Quantification to measure the difference in overexpression levels of the At-*ESI2* gene was done using visual estimation of PCR products obtained by agarose gel electrophoresis stained with ethidium bromide (Figure 1).

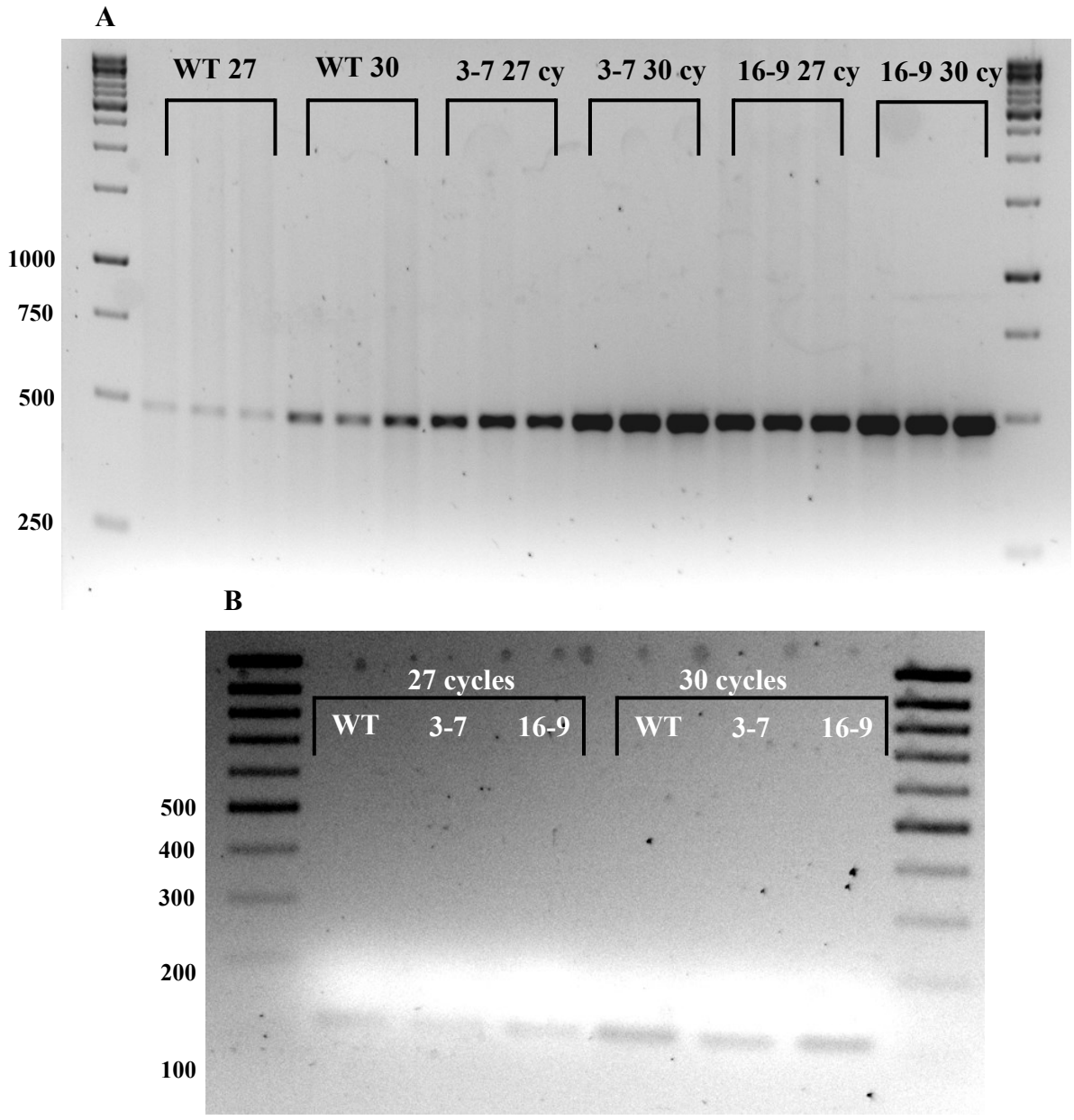

Figure 1. A. Analysis by RT-PCR of At-*ESI2* expression in *Arabidopsis* wild type Columbia-0 and transgenic lines overexpressing the gene under the regulation of the 35S promoter. Specific PCR fragments of about 490 bp were detected. *Lanes 1-6*: At-*ESI2* expression in WT-Col-0 *Arabidopsis* plants with 27 and 30 cycles of amplification, *lanes1-3* and *4-6*, respectively. *Lanes 7-12*: At-ESI2 expression in OE transgenic *Arabidopsis* plant line 3-7 with 27 and 30 cycles of PCR amplification, l*anes 7-9* and *10-12*, respectively. *Lanes 13-18*: AtESI2 expression in transgenic OE line 16-9 with 27 and 30 cycles of amplification, l*anes 13-15* and *16-18*, respectively.
B. Actin control to show equal amounts of first strand cDNA in WT Columbia-0 lines, as well as 3-7 and 16-9 transgenic *Arabidopsis* lines. *Lanes 1-3*: RT-PCR at 27 cycles. *Lanes 4-6*: RT-PCR at 30 cycles

7. *Arabidopsis thaliana* T-DNA Insertion Mutant Plants

A. thaliana T-DNA insertion mutant lines SALK 142954, SALK 142962, and SAIL_437_B03 were obtained from the ABRC Stock Centre, Ohio State University. The plant DNA was extracted using the Extract-N-Amp Plant Kit (Sigma). The DNA was then PCR amplified using primers recommended by the SALK Institute primer design tool, SIGnAL (http://signal.salk.edu/cgi-bin/tdnaexpress) to verify the presence of the T-DNA and to identify homozygous lines. The insertions were located in, or upstream of the At-*ESI2* gene.

PART III: RESULTS

1. Identification of Potential Homologs of *Triticum aestivum* Genes *ESI2* and *Ran1* in *Arabidopsis*

The Ta-*Esi2* gene from *T. aestivum* encodes a 321 amino acid protein with a 97% identity to genes in *Lophopyrum elongatum* (GI:62861393), and 75% identity with the most similar gene in *Brachypodium distachyon* (GI:357123444), but showed little similarity to any genes in *Arabidopsis*. However, the 125 aa copper-binding domain of the wheat *Esi2* showed a 67% amino acid sequence similarity to one gene in *Arabidopsis*, At4g27520, referred to as At-*ESI2*. The C-terminal half of the protein encoded by Ta-

Esi2 contains a region with approximately 140 amino acids made up of several tandem repeats of a motif rich in methionine, serine, and proline. At-*ESI2* also contains repeated motifs in the C-terminal region; these are rich in lysine, serine, proline, and glutamine though the sequence of the motif does not have significant similarity to that of Ta-*Esi2*.

A BLAST search identified the wheat Ta-*Ran* homeolog in Arabidopsis (At4g27520), referred to as At-*RAN*. The two proteins share 94% amino acid sequence identity.

2. Protein-Protein Interaction of ESI2 and Ran

2.1 His_6-tag Pull-Down Assay

A His_6-tag pull-down assay was done using Ta-Esi2 as bait to confirm the interaction with the Ta-Ran proteins and to compare the relative binding of the two proteins when Ta-Ran is in the active GTP-bound, and inactive GDP-bound state. Ta-Esi2-GST (59 kDa) was found to interact *in vitro* with Ta-Ran-His_6 (26 kDa) in both the GDP- and GTP-bound states (Figure 2, lanes A and B). Surprisingly, there seemed to be no preference for one state over the other, as equal amounts of Esi2 were found to interact with both the GDP- and GTP-bound forms of Ran. The control, Ta-Ran-His_6 incubated with GST beads, (Figure 2, lane C) did not show any interaction.

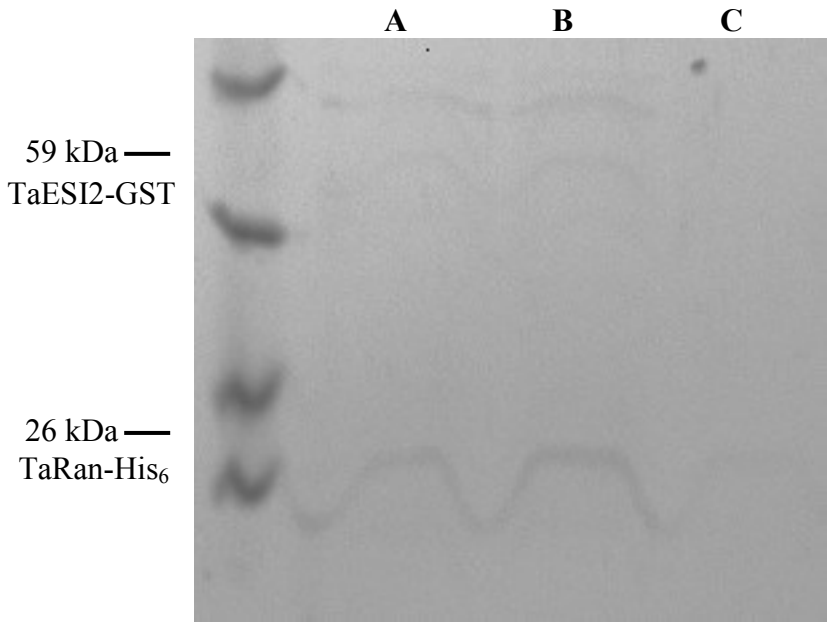

Figure 2. *In vitro* interaction of TaRan-His_6 and TaESI2-GST via His_6-tag pull-down assay and SDS-PAGE. A**.** TaRan-His_6 immobilized on Ni-NTA Agarose beads and preloaded with GDP in lysate with 200 mM $MgCl_2$ was incubated for 2 h at 4ºC with 1 ml of TaESI2-GST. **B.** TaRan-His_6 immobilized on Ni-NTA Agarose beads and preloaded with GTP in lysate with 200 mM $MgCl_2$ was incubated for 2 h at 4ºC with 1 ml of TaESI2-GST. **C.** Control. TaRan-His_6 incubated with GST beads.

3. Sub-Cellular Protein Localizations of At-ESI2 and At-RAN

At-ESI2 and At-RAN were expressed as green fluorescent fusion proteins, At-ESI2::eGFP and At-RAN::eGFP, respectively, in *Nicotiana benthamiana* leaf epidermal cells and viewed under a confocal microscope with the tonoplast marker. At-RAN::eGFP localized to the nucleus (Figure 3). The nucleus is distinguishable in tobacco leaves as a large, circular organelle between the plasma membrane and tonoplast. To verify the area of localization, both At-Ran::eGFP and At-ESI2::eGFP were co-localized with the tonoplast marker (Figures 3 and 4, respectively). At-ESI2::eGFP was seen to localize to the tonoplast (vacuolar membrane) (Figure 4).

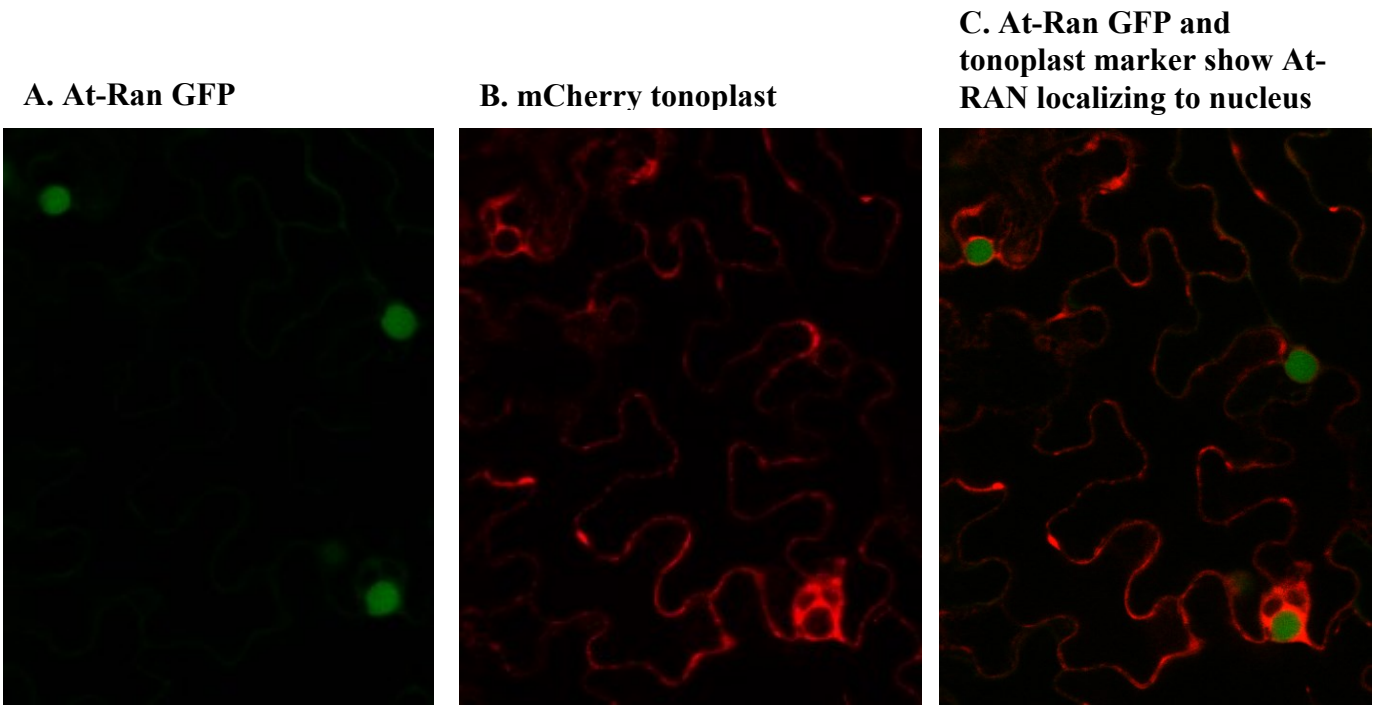

Figure 3. Cross-section image of *N. benthamiana* leaves, transiently transformed with Agrobacterium tumefaciens showing localization of AtRan::eGFP to the nucleus, co-expressed with the tonoplast marker, gammaTIP::mCherry.

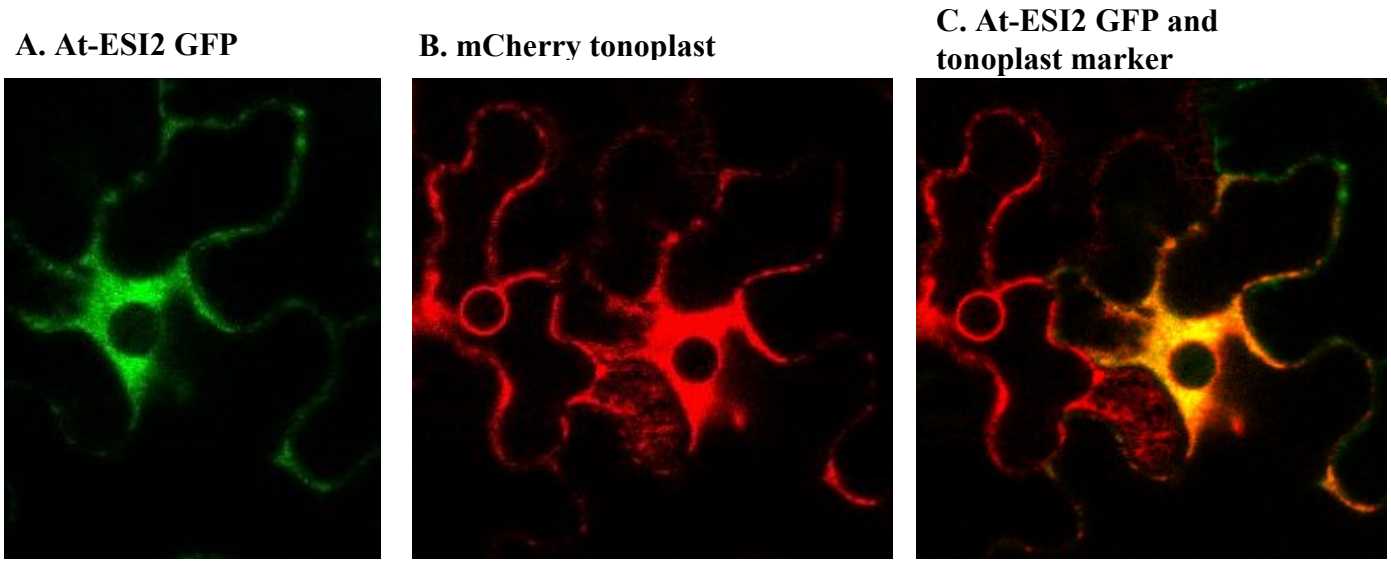

Figure 4. Cross-section image of *N. benthamiana* leaves, showing localization of AtESI2::eGFP to the tonoplast, co-expressed with the tonoplast marker, gammaTIP::mCherry.

4. *In vivo* Protein-Protein Interactions of Ta-Esi2, Ta-Ran1, At-ESI2 and At-RAN

BiFC was used to test the interaction between the Arabidopsis ESI2 and Arabidopsis RAN. At-ESI2 was fused to the carboxy portion of eYFP (At-ESI2::eYFP-C), while At-RAN was fused to the amino portion of eYFP (At-RAN::eYFP-N). Constructs were then expressed together in the same cell with the gammaTIP::mCherry tonoplast marker. The interaction between the Arabidopsis ESI2 and RAN showed localization to the cytoplasm and possibly the tonoplast (Figure 5). The localization was seen surrounding the nucleus and on the periphery of tobacco cells. A comparison with the localization of the tonoplast marker, gammaTIP::mCherry (Figure 6), indicates that localization was also seen across what we have termed "cytoplasmic bridges", shown in Figure 5 and 6 with arrows. These bridges have been described as "occasional transvacuolar strands [that] seem to bisect the vacuole; these represent cytoplasmic tunnels that traverse the lumen of the continuous vacuole" (Nelson 2007). The localization was specific to the cytoplasm and cytoplasmic bridges, and possibly the tonoplast, with no labelling appearing in the nucleus or other organelles. Interaction between Ta-Ran::eYFP-N and Ta-Esi2::eYFP-C was also seen along the edges of tobacco cells (Figure 7A). Cell wall staining with propidium iodide (Figure 7B) revealed that the interaction did not occur within the cell wall, but was most likely along the edge of the tonoplast or plasma membrane. The Arabidopsis RAN protein expressed as a fusion to the full length eGFP, At-RAN::eGFP, was seen to localize to the nucleus in tobacco cells (Figure 3). The nucleus was easily distinguishable as a large circular organelle pressed between the tonoplast and the plasma membrane. At-ESI2::eGFP was shown to localize heavily around the nucleus and also along the periphery of the cell (Figure 4). The eGFP

label overlapped with the tonoplast marker, gammaTIP::mCherry, but the distribution of the marker did not appear entirely tonoplastic, since the labelling around the nucleus appeared associated with a membrane, but appeared to be cytoplasmic.

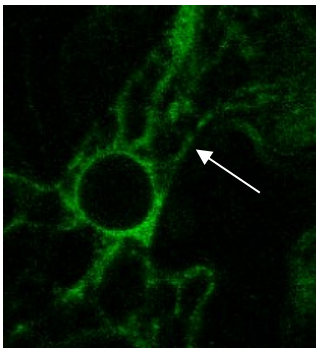

Figure 5. Cross-section image of *N. benthamiana* leaves, showing localization of the AtRan::eYFP-N and AtESI2::eYFP-C BiFC interaction to the tonoplast, with little or no expression inside the nucleus. Cytoplasmic bridges are shown with an arrow.

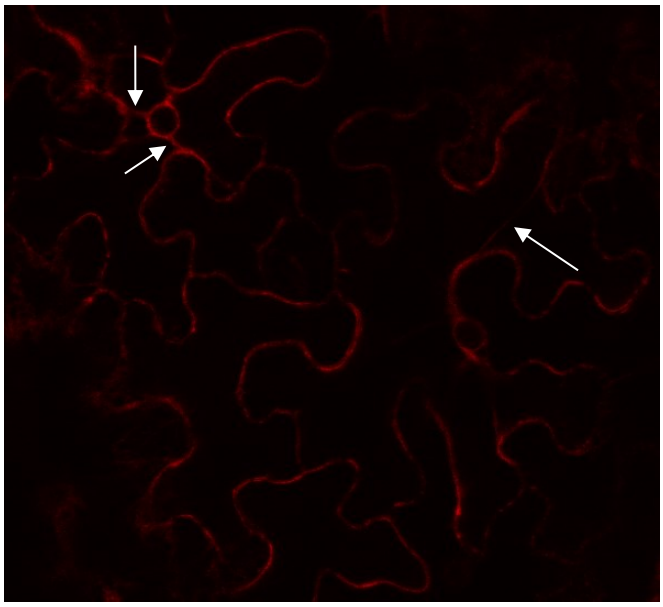

Figure 6. Cross-section image of *N. benthamiana* leaves, showing localization of the tonoplast marker, gammaTIP::mCherry. Cytoplasmic bridges are shown with arrows.

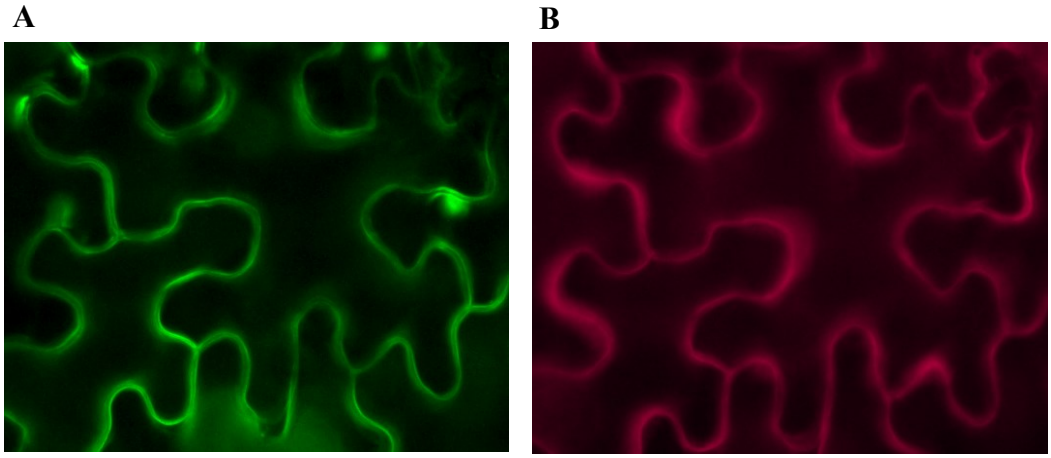

Figure 7. A. Cross-section image of *N. benthamiana* leaves, showing localization of the TaRan::eYFP-N and TaESI2::eYFP-C BiFC interaction outside of the cell wall under Zeiss Axioplan fluorescence microscope (Carl-Zeiss, Germany).
B. Cross-section image of *N. benthamiana* leaves, showing staining of cell wall with propidium iodide interaction under Zeiss Axioplan fluorescence microscope (Carl-Zeiss, Germany).

5. *Arabidopsis thaliana ESI2* mutant plants

Three seed lines with potential T-DNA insertional mutations of the *Arabidopsis thaliana* At-*ESI2* gene, AT4G227520, were selected and screened. Lines SALK_142954, SALK_142962, and SAIL_437_B03 had been identified at the SIGnAL T-DNA Express public database (http://signal.salk.edu/cgi-bin/tdnaexpress) as having T-DNA insertions within the coding portion of the At-*ESI*2 gene. Line SALK_142962 has been identified in the T-DNA Express database as a line with a T-DNA insertion within the promoter of the At-*ESI*2 gene. Four heterozygous plants with the T-DNA insertion were identified. PCR amplification using primers LBb1.3 and RB yielded a 500 bp product in plants carrying the T-DNA insertion and amplification using gene specific LB-RB primers yielded a 968 bp product in heterozygous plants and plants lacking the insertion. For line SALK_142954, LBb1.3 and RB primers yielded a 600 bp product in plants carrying the

T-DNA insertion, and amplification using gene specific LB-RB primers yielded a 1194 bp product in heterozygous plants and plants lacking the insertion. However, the absence of a PCR band, normally taken as evidence for the lack of a gene or insertion DNA, was considered unreliable since the verification of a heterozygous line that should yield both a 1194 and a 600 bp band was not found in the segregating population. Both the 1194 bp and the 600 bp bands were observed separately in different plants, but never together in the same plant. This raised doubt about the reliability of the PCR assay.

6. Overexpression of the *ESI2* gene in *Arabidopsis thaliana*

From the twenty-three T_2 lines, lines 3 and 16 were observed to have multiple insertions (15:1 ratio of GFP to no-GFP, respectively, in the T_2 generation). From these lines, offspring T_3 plants 3-7, 3-9, 3-10, 3-12, 16-5 and 16-9 were shown to be homozygous for at least one locus, since 100% of the seeds from these plants showed GFP fluorescence in the seed coat (Figure 8B), compared to wild type Columbia-0 seed (Figure 8A). In a line with multiple insertions, it is not possible to identify individuals that are homozygous at all loci by observing GFP expression in the seed because the trait is dominant, and homozygosity at the one locus masks heterozygosity or a null state at the other locus. Line 6 was shown to have a single insertion, as it has a heterozygous 3:1 segregation in the T_2 seed (Figure 8C). From the T_2 plant, line 6-9 was shown to be homozygous since all of the T_3 seed had uniform GFP fluorescence. Lines 12 and 23 also appeared to have single insertions. Line 12 had many heterozygous offspring and one line, 12-2, was homozygous. Line 23 had two heterozygous T_2 offspring.

RT-PCR was used to test the level of overexpression of the At-*ESI2* gene in Arabidopsis. Lines 3-7 and 16-9 were shown to have five times the level of expression of the At-*ESI2* gene compared to the wild type (Figure 1). However, there was no observable difference in time to germination, time to flowering, or leaf number in 35S::AtESI2 *Arabidopsis* plants used for phenotypic analysis.

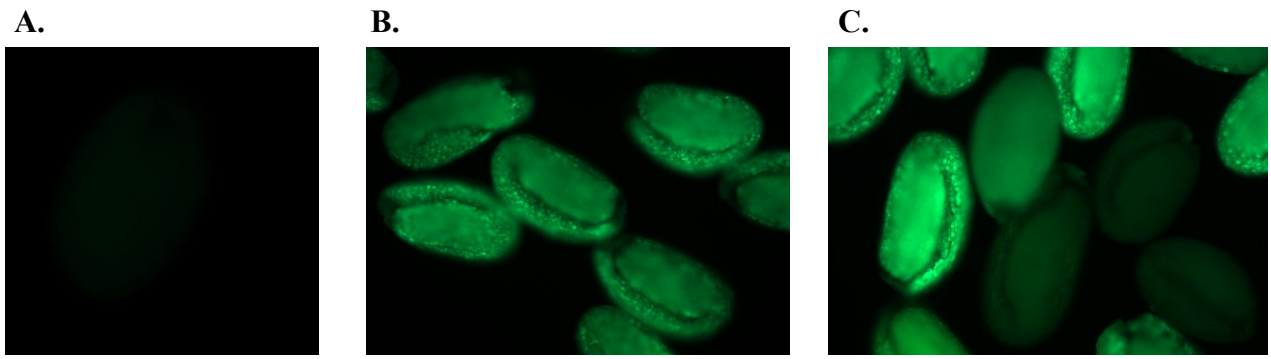

Figure 8. GFP fluorescence from transgenic seed expressing 35S::AtESI2 with the OLE1-GFP marker. **a.** Wild type Columbia-0 seed. **b.** T_3 seed from homozygous line 3-9. **c.** T_3 seed from heterozygous line 6-8 showing a 3:1 ratio of, indicating a single insertion in the T_2 parent.

PART IV. DISCUSSION

The aim of this thesis was an examination of the plant proteins involved in the stress response of *Arabidopsis thaliana* and *Triticum aestivum*. An in-depth characterization of the protein-protein interactions between the *RAN* and *ESI2* genes, as well as a phenotypic analysis of the overexpression of *ESI2* in Arabidopsis, has laid a foundation for the characterization of the roles of these genes in a plant stress response.

1. Interactions between *ESI2* and *RAN*

The data from the His_6-tag pull down assay revealed an equal affinity between wheat Esi2 and the wheat Ran in either the GDP- or GTP-bound form. This provided

evidence to support the previously reported interaction between wheat Esi2 and Ran based on a yeast two-hybrid screen (Tardiff *et al.* 2007). Further examination of the amino acid sequences of Ta-*Esi2* and At-*ESI2* revealed a similar copper-binding domain and repeated sequence motifs. Additionally, a hydropathy plot (Figure 9) comparing the sequences of Ta-*Esi2* (Figure 9A) and At-*ESI2* (Figure 9B) revealed similar patterns of hydrophobicity and hydrophilicity.

The interaction between *ESI2* and *RAN* was further characterized via BiFC analysis in *N. benthamiana* cells. BiFC results showed At-ESI2 interacting with At-RAN outside of the nucleus along the edge of the vacuole, in the tonoplast and cytoplasm. Additionally, Ta-Esi2 and Ta-Ran were shown to interact along the periphery of tobacco cells, also potentially within the tonoplast or cytoplasm. However, in the absence of At-ESI2, At-RAN was shown to localize almost exclusively to the nucleus. It is clear that the interactions between ESI2 and RAN are outside the nucleus, and suggests that ESI2 may sequester Ran outside the nucleus. However, the assays used here do not determine the net effect on the distribution of RAN between the nucleus and the cytoplasm. Further work is required to determine if high levels of ESI2 expression affect RAN levels inside the nucleus. Some insight into this could be gained by simultaneous ectopic expression of the two proteins as fusions to full-length fluorescent proteins such as eGFP and mCherry.

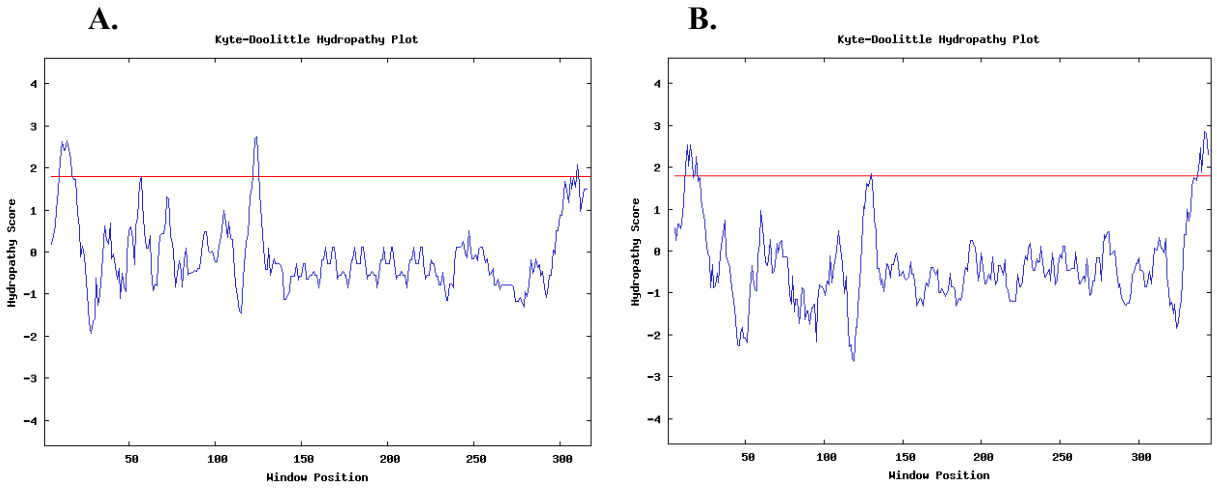

Figure 9. Kyte-Doolittle hydropathy plot. **A.** Kyte-Doolittle hydropathy plot of Ta-*Esi2*. **B.** Kyte-Doolittle hydropathy plot of At-*ESI2*.

2. Phenotype of At-*ESI2* Overexpression in *Arabidopsis thaliana*

The preliminary data indicate that the overexpression of the At-*ESI2* gene in transgenic *Arabidopsis* plants does not have a phenotypic effect on germination, time to flowering, or leaf number. Preliminary data, not presented here, on root growth did not detect clear differences in root elongation or branching between At-*ESI2* overexpressing plants and WT Columbia control. However, more detailed studies of lateral root number and time to emergence, as well as the effect of different types of stress, have yet to be carried out.

It has previously been shown that levels of *ESI2* increase rapidly during a plant stress response (Gulick et al. 2005). Since *RAN* is a known regulator and has been shown to play a role in the plant stress response, it is possible that *ESI2* regulates *RAN* by competing with importins to bind free Ran in the cytoplasm. This would reduce levels of

transport of proteins out of the nucleus, and help regulate such factors as root length, cell growth and division, or stomate opening/closing during a stress response. After binding to *RAN*, *ESI2* may affect functions that *RAN* is known to control, such as nuclear transport and cell division. A mutation locking *RAN* in its GDP-bound form (T24N mutant) in *Xenopus* extracts prevented plant cells from entering mitosis by directly blocking DNA replication (Kornbluth *et al.* 1994). Furthermore, it is thought that changes in *RAN* expression may indirectly disrupt cell division by interfering with proteins required for the G2 to mitosis cell cycle transition (Wang *et al.* 2006). For example, the cytosolic B1-type cyclin must be carried into the nucleus by *RAN*-driven transport so the cyclin can bind to chromosomes and initiate the cell transition into mitosis (Inze 2005). Additionally, an increase in RanGDP has been shown to cause an activation of the cell spindle checkpoint (Musacchio and Hardwick 2002). Thus, *ESI2* may function in regulating *RAN* by a regulation of the guanosine phosphates that bind *RAN* or in the localization of *RAN* and play a direct role in cell growth and division.

There are three main pathways through which a plant can evoke a stress response: a) homeostasis, including osmotic homeostasis or osmotic adjustment, usually in response to salt stress, b) detoxification, including damage control and repair, and c) management of growth (Zhu 2002). These result in a variety of phenotypic changes, including rapid reduction in the elongation of leaves (Fricke *et al.* 2006), changes in shoot growth, and increased stomatal closure (Knight and Knight 2001). Root structure exhibits a slightly different response than the rest of the plant, and may continue to elongate under mild conditions of stress (Pardo 2010). Such a diverse variety of responses to stress conditions indicates an intricate and complex network behind a plant stress response. Any new

discoveries that reveal new levels of interactions would bring scientists one step closer to completing a full map of the stress response pathway in plants. However, the overexpression of At-*ESI2* did not cause altered growth or development over the period of observation, thus this work did not provide evidence that *ESI2* overexpression affected these characteristics. Yet it is possible that *ESI2* may be part of a more complex interaction network that manages to circumvent the effects of overexpression. As such, other means of study would be necessary to characterize the effects of *ESI2* on *RAN*.

3. Future Work

The role of *ESI2* as a part of a *RAN*-mediated plant stress response is an area that requires further examination. Future research on the effect of *ESI2* on the intracellular localization of *RAN* both inside and outside the nucleus would provide further insight into the potential role of *ESI2* in sequestering *RAN* in the cytoplasm. Additional observations of the effects of *ESI2* overexpression on cell division, either by measuring growth rates in yeast, or in HeLa cells, could prove revealing. If an effect were observed, microscopic analysis of aster formation or the G2/mitosis checkpoint could be carried out. Finally, the additional phenotypic analysis of At-*ESI2* overexpression plants under stress conditions to help reveal the pathways *ESI2* might be operating in will help to further elucidate its function in the *RAN*-mediated plant stress response. Down-regulation or knockout of At-*ESI2* via RNAi could provide further insight into the phenotypic effects and subsequent role of At-*ESI2* in the plant stress response system.

Since *ESI2* is known to be up-regulated during times of stress, additional phenotypic analysis in the leaves or roots under conditions of stress could prove

beneficial. The *Arabidopsis* eFP Browser from the University of Toronto (http://bar.utoronto.ca/efp_arabidopsis/cgi-bin/efpWeb.cgi) which has extensive data on gene expression patterns, shows significant up-regulation of At-*ESI2* (At4g27520) after one hour of osmotic stress, one hour of 200 mM NaCl stress, and after one hour of 100 μm of ABA treatment. A phenotypic analysis under these stress conditions may help to reveal the role of *ESI2* in a stress response and subsequently help to uncover the nature and biological importance of its interactions with the *RAN* gene.

PART V. REFERENCES

Alonso, J.M. *et al*. (2003) Genome-wide insertional mutagenesis of Arabidopsis thaliana. Science, 1, 653 – 657.

Arabidopsis Genome Initiative. (2002) Analysis of the genome sequence of the flowering plant Arabidopsis thaliana. Nature, 408, 796 – 815.

Benson, D.A., Karsch-Mizrachi, .I, Lipman, D.J., Ostell, J. and Wheeler D.L. (2005) GenBank. Nucleic Acids Res. 33, 34 – 38.

Bent, A. (2006) Arabidopsis thaliana floral dip transformation method. Methods Mol. Biol. 343, 87 – 103.

Berkman, P.J. et al. (2013) Dispersion and domestication shaped the genome of bread wheat. Plant Biotechnol. 1, 1 – 8.

Bray, E.A., Bailey-Serres, J. and Weretilnyk, E. (2000) Responses to abiotic stresses. Biochemistry and molecular biology of plants. American Society of Plant Physiologists, Rockville, MD, 1158 – 1249.

Chantret, N. et al. (2005) Molecular basis of evolutionary events that shaped the hardness locus in diploid and polyploid wheat species (Triticum and Aegilops). Plant Cell, 17, 1033 – 1045.

Chinnusamy, V., Gong, Z. and Zhu, J.K. (2008) Nuclear RNA export and its importance in abiotic stress responses of plants. Curr. Top Microbiol. Immunol. 326, 235 – 255.

Clough, S.J. and Bent, A.F. (1998) Floral dip: a simplified method for Agrobacterium-mediated transformation of Arabidopsis thaliana. Plant J. 16, 736 – 743.

Dasso, M. (2001) Running on Ran: Nuclear Transport and the Mitotic Spindle. Cell, 104, 321–324.

Dasso, M. (2002) The Ran GTPase: Theme and Variations. Curr. Biol. 12, 502 – 508.

English, J.J., Mueller, E. and Baulcombe, C. (1996) Suppression of Virus Accumulation in Transgenic Plants Exhibiting Silencing of Nuclear Genes. Plant Cell, 8, 179 – 188.

Food and Agriculture Organisation of the United Nations (2012) FAOSTAT Food Supply – Crops Primary Equivalent.

Fricke, W., Akhiyarova, G., Wei, W., Alexandersson, E., Miller, A., Kjellbom, P.O., Richardson, A., Wojciechowski, T., Schreiber, L., Veselov, D., Kudoyarova, G., Volkov, V. (2006) The short-term growth response to salt of the developing barley leaf. J Exp Bot. 57, 1079 – 1095.

Galvez, A.F., Gulick, P.J. and Dvorak, J. (1993) Characterization of the Early Stages of Genetic Salt-Stress Responses in Salt-Tolerant *Lophopyrum elongatum*, Salt-Sensitive Wheat, and Their Amphiploid. Plant Physiol. 103, 257 – 265.

Görlich, D. and Kutay, U. (1999) Transport Between the Cell Nucleus and the Cytoplasm. Cell Dev. Biol. 15, 607 – 660.

Görlich, D., Seewald, M.J. and Ribbeck, K. (2003) Characterization of Ran-driven cargo transport and the RanGTPase system by kinetic measurements and computer simulation. EMBO J. 22, 1088 – 1100.

Gruss, O.J., Carazo-Salas, R.E., Schatz, C.A., Guarguaglini, G., Kast, J., Wilm, M., Le Bot, N., Vernos, I., Karsenti, E. and Mattaj, I.W. (2001) Ran induces spindle

assembly by reversing the inhibitory effect of importin alpha on TPX2 activity. Cell, 104, 83 – 93.

Gulick, P.J. and Dvorak, J. (1992) Coordinate Gene Response to Salt Stress in *Lophopyrum elongatum*. Plant Physiol. 100, 1384 – 1388.

Gulick, P.J., Drouin, S., Yu, Z., Danyluk, J., Poisson, G., Monroy, A. and Sarhan, F. (2005) Transcriptome comparison of winter and spring wheat responding to low temperature. Genome, 48, 913 – 923.

Haizel, T., Merkle, T., Pay, A., Fejes, E. and Nagy, F. (1997) Characterization of proteins that interact with the GTP-bound form of the regulatory GTPase Ran in Arabidopsis. Plant J. 11, 93 – 103.

Hasegawa K., Ryu, S.J. and Kaláb, P. (2013) Chromosomal gain promotes formation of a steep RanGTP gradient that drives mitosis in aneuploid cells. J Cell Biol. 200, 151 – 161.

Heim, R., Cubitt, A.B. and Tsien, R.Y. (1995) Improved green fluorescence. Nature, 373, 663 – 664.

Hu, C. D., Chinenov, Y. and Kerppola, T.K. (2002) Visualization of interactions among bZIP and Rel Family proteins in living cells using bimolecular fluorescence. Mol. Cell, 9, 789 – 798.

Huang, A.H. (1996) Oleosins and Oil Bodies in Seeds and Other Organs. Plant Physiol. 110, 1055 – 1061.

Inze, D. (2005) Green light for the cell cycle. EMBO J. 24, 657 – 662.

Kahana, J.A. and Cleveland, D.W. J Cell Biol. (1999) Beyond nuclear transport. Ran-GTP as a determinant of spindle assembly. J Cell Biol. 146, 1205 – 1210.

Karimi,,M., Inzé, D. and Depicker, A. (2002) GATEWAY vectors for Agrobacterium-mediated plant Transformation. Trends Plant Sci. 7, 193 – 195.

Kim, S.H., Arnold, D. Lloyd, A. and Roux, S.J. (2001) Antisense Expression of an Arabidopsis Ran Binding Protein Renders Transgenic Roots Hypersensitive to Auxin and Alters Auxin-Induced Root Growth and Development by Arresting Mitotic Progress. Plant Cell, 13, 2619 – 2630.

Knight, H. and Knight, M.R. (2001) Abiotic stress signaling pathways: specificity and cross-talk. Trends Plant Sci. 6, 262 – 267.

Kornbluth, S., Dasso, M. and Newport, J. (1994) Evidence for a Dual Role for TC4 Protein in Regulating Nuclear Structure and Cell Cycle Progression. J Cell Biol. 125, 705 – 719.

Li, Y., Sierra, A.M., Ai, H.W. and Campbell, R.E. (2008) Identification of sites within a monomeric red fluorescent protein that tolerate peptide insertion and testing of corresponding circular permutations. Photochem Photobiol. 84, 111 – 119.

McFadden, E.S. and Sears, E.R. (1946) The origin of Triticum spelta and its freethreshing hexaploid relatives. J. Hered. 37, 81 – 107.

Merkle, T. (2011) Nucleo-cytoplasmic transport of proteins and RNA in plants. Plant Cell Rep. 30, 153 – 176.

Meyerowitz, E.M. (2001) Prehistory and History of Arabidopsis Research. Plant Physiol. 125, 15 – 19.

Musacchio, A. and Hardwick, K.G. (2002) The spindle check-point: Structural insights into dynamic signaling. Nat Rev Mol Cell Biol. 3, 731 – 741.

Nelson, B.K., Cai, X. and Nebenführ, A. (2007) A multicolored set of in vivo organelle markers for co-localization studies in Arabidopsis and other plants. Plant J. 51, 1126 – 1136.

Ormö, M., Cubitt, A.B., Kallio, K., Gross, L.A., Tsien,R.Y. and James, S. (1996) Remington Crystal Structure of the Aequorea victoria Green Fluorescent Protein. Science, 273 1392 – 1395.

Pardo, J.M. (2010) Biotechnology of water and salinity stress tolerance. Curr Opin in Biotechnol. 21, 185– 196.

Pitman, M, and A Lauchli. *Salinity: Environment - Plants - Molecules. Global Impact Of Salinity And Agricultural Ecosystems*. 1st ed. United States: Kluwer Academic Publishers, 2002. 3 – 20. Print.

Shaner, N.C., Campbell, R.E., Steinbach, P.A., Giepmans, B.N.G., Palmer, A.E. and Tsien, R.Y. (2004) Improved monomeric red, orange and yellow fluorescent proteins derived from *Discosoma* sp. Red fluorescent protein. Nature Biotech. 22, 1567 – 1572.

Shi, X., Basran, J., Seward, H.E., Childs, W., Bagshaw, C.R. and Boxer, S.G. (2007) Anomalous Negative Fluorescence Anisotropy in Yellow Fluorescent Protein (YFP 10C): Quantitative Analysis of Fret in YFP Dimers. Biochem. 46, 14403 – 14417.

Shimada, T.L., Shimada, T., Takahashi, H., Fukao, Y. and Hara-Nishimura, I. (2008) A novel role of oleosins in freezing tolerance of oilseeds in Arabidopsis thaliana. Plant J. 55, 798 – 809.

Shimada, T.L., Shimada, T. and Hara-Nishimura, I. (2010) A rapid and non-destructive screenable marker, FAST, for identifying transformed seeds of Arabidopsis thaliana. Plant J. 61, 519 – 528.

Sparkes, I.A., Runions, J., Kearns, A. and Hawes, C. (2006) Rapid, transient expression of fluorescent fusion proteins in tobacco plants and generation of stably transformed plants. Nature Prot. 1, 2019 – 2025.

Tardiff, G., Kane, N.A., Adam, H., Labrie, L., Major, G., Gulick, P., Sarhan, F. and Laliberte, J.F. (2007) Interaction network of proteins associated with abiotic stress response and development in wheat. Plant Mol. Biol. 63, 703 – 718.

Todorova, R. (2009) In vitro interaction between the N-terminus of the Ewing's sarcoma protein and the subunit of RNA polymerase II hsRPB7. Mol Biol. Rep. 36, 1269 – 1274.

Vernoud V., Horton A.C., Yang Z. and Nielsen E. (2003) Analysis of the small GTPase gene superfamily of Arabidopsis. Plant Physiol. 131, 1191–208.

Voinnet O., Rivas S., Mestre P. and Baulcombe D.C. (2003) An enhanced transient expression system in plants based on suppression of gene silencing by the p19 protein of tomato bushy stunt virus. Plant J. 33, 949 – 956.

Wang, X., Xu, Y., Han, Y., Bao, S., Du, J., Yuan, M., Xu, Z. and Chong, K. (2006) Overexpression of *Ran1* in Rice and Arabidopsis Alters Primordial Meristem, Mitotic Progress, and Sensitivity to Auxin. Plant Physiol. 140, 91 – 101.

Wanjugi, H., Coleman-Derr, D., Huo, N., Kianian, S.F., Luo, M.-C., Wu, J., Anderson, O. and Gu, Y.Q. (2009) Rapid development of PCR-based genome specific repetitive DNA junction markers in wheat. Genome, 52, 576 – 587.

Wesley, S.V. *et al*. (2001) Construct design for efficient, effective and high-throughput gene silencing in plants. Plant J. 27, 581 – 590.

Xu, X.M., Zhao, Q., Rodrigo-Peiris, T., Brkljacic, J., He, C.S., Müller, S. and Meier, I. (2008) RanGAP1 is a continuous marker of the Arabidopsis cell division plane. Proc. Natl Acad. Sci. USA, 18637 – 18642.

Zang, A., Xu X., Neill, S. and Cai, W. (2010) Overexpression of OsRan2 in rice and Arabidopsis renders transgenic plants hypersensitive to salinity and osmotic stress. J Exp. Bot. 61, 777 – 789.

Zhang, H. and Dawe, R.K. (2011) Mechanisms of plant spindle formation. Chrom. Res. 19, 335 – 344.

Zhu, J. (2002) Salt and Drought Stress Signal Transduction in Plants. Annu Rev Plant Biol. 53, 247 – 273.

Zimmer, M. (2009) GFP: from jellyfish to the Nobel prize and Beyond. Chem. Soc. Rev. 38, 2823 – 2832.

Appendix I

Oligonucleotide PCR primers used in this study:

Primer	Description	Sequence (5' → 3')[1]
N02*att*B1	*Esi2-2* Forward Gateway Primer	GGGGACAAGTTTGTACAAAAAAGCAGGCTCC ATGGCGAGTCCTCGCGGTCTGG
N02*att*B2	*Esi2-2* Reverse Gateway Primer	GGGGACCACTTTGTACAAGAAAGCTGGGTC GATAGCGAGCATGGCGTAGCC
RlGBattB1F	*Ran*1 Forward Gateway Primer	GGGGACAAGTTTGTACAAAAAAGCAGGCTCC ATGGCGCTGCCGAACCAGAAC
RlGBattB1R	*Ran*1 Reverse Gateway Primer	GGGGACCACTTTGTACAAGAAAGCTGGGTC CTCGATCAGATCGTCATCGTC
AtRan2FPGW	At-*RAN2* Forward Primer Gateway	GGGGACAAGTTTGTACAAAAAAGCAGGCTTC ATGGCTCTACCTAACCAACAAAC
AtRan2RPGW	At-*RAN2* Reverse Primer Gateway	GGGGACCACTTTGTACAAGAAAGCTGGGTC CTCAAATGCGTCATCATCATC
AtESI2cDNAFP1	At-*ESI2* cDNA Forward Primer for RTPCR	GCACCACCTAAATCCACGTC
AtESI2cDNARP1	At-*ESI2* cDNA Reverse Primer for RTPCR	TCAAACTGGGATCCAAAAACA
AtESI2GUSFP	Promoter of At-*ESI2* with GUS fusion Forward Primer	GGGGACAAGTTTGTACAAAAAAGCAGGCTTC GGGAGAAGAACACGTGGCTAA
AtESI2GUSRP2	Promoter of At-*ESI2* with GUS fusion Reverse Primer2	GGGGACCACTTTGTACAAGAAAGCTGGGTC CACCTCTAGCACCGAGTCAGC
AtESI2FPGW	At-*ESI2* Forward Gateway Primer	GGGGACAAGTTTGTACAAAAAAGCAGGCTTC ATGACCTTTCTAAAAATGAAAAGC
AtESI2RPGWstop	At-*ESI2* Reverse Gateway Primer with STOP codon	GGGGACCACTTTGTACAAGAAAGCTGGGTC TTAAGCTGACAGAAAGATGGTCAA
AtESI2RPGWnostop	At-*ESI2* Reverse Gateway Primer without STOP codon	GGGGACCACTTTGTACAAGAAAGCTGGGTC AGCTGACAGAAAGATGGTCAA

[1] Underlined sequences are *attB* sites used for Gateway Cloning